ELSEVIER

Journal of Nuclear Materials 302 (2002) 96–103

journal of nuclear materials

www.elsevier.com/locate/jnucmat

Concentration dependent diffusion of carbon in tungsten

K. Schmid *, J. Roth

Max-Planck-Institut für Plasmaphysik, EURATOM-Association, Boltzmannstrasse. 2, D-85748 Garching, Germany

Received 10 September 2001; accepted 15 February 2002

Abstract

This paper concerns with the concentration dependence of the C diffusion in W. An effective, concentration dependent diffusion coefficient $D(C)$ was used to model the diffusion of C in W in the temperature range from 1000 to 1100 K. $D(C)$ was thereby determined experimentally by a Boltzmann–Matano analysis of depth profiles taken from C–W diffusion couples. In cases where this analysis was not applicable, additional values for $D(C)$ were also obtained by iteratively fitting measured depth profiles using the diffusion code DIFFUSEDC and adjusting $D(C)$ accordingly. All depth profiles were measured using Rutherford backscattering. The effective diffusivities were found to be below the limits of the method used ($<10^{-22}$ m^2/s) for temperatures below 1000 K. Between 1000 and 1100 K they are in the order of 10^{-19} m^2/s and strongly dependent on the C concentration. This concentration dependence exhibits a sharp drop of approximately one order of magnitude for C concentrations larger than 20–40%.

1. Introduction

In modern fusion devices the surface of the first plasma facing wall consists of a mixture of various materials. Graphite and CFC materials are used for high heat load components, high-Z refractory materials or low-Z metals as wall cladding and the surface is frequently conditioned by applying B, Si or Be coatings [1]. Post-mortem analysis of wall components reveals surface layers consisting of a mixture of all materials. Their formation is governed by implantation of hydrogen and impurity species followed by diffusion of these implanted particles into the hot wall material. The composition resulting from these processes determines important wall characteristics like erosion and hydrogen isotope inventory. Therefore, it is important to be able to model the basic mechanisms, such as the diffusion of impurities.

The first wall of future devices will be made from the materials W, C and Be. For instance in the current ITER design [2] the divertor will be made from C and W whereas the rest of the first wall will be made from Be. The W tiles in the divertor chamber are exposed to high heat and carbon impurity fluxes which will lead to high C concentrations in the W. The evolution of the implanted C is mainly governed by diffusion and the formation of carbides [3]. Diffusion data for C in W is sparse and is mainly determined for very low C concentrations and rather high temperatures [4]. This work tries to determine the diffusion coefficient in a wide range of concentrations and at temperatures occurring at the first wall of fusion devices from the analysis of C depth profiles in W.

To model diffusion with a concentration dependent diffusion coefficient we solve the general form of Fick's second law. Solving this equation for arbitrary starting and boundary conditions cannot be done analytically. Therefore we use the new program DIFFSEDC to solve the equation numerically applying a simple finite difference approach [5]. For special boundary conditions the concentration dependent diffusion coefficient, $D(C)$, can be extracted from measured depth profiles using the Boltzmann–Matano analysis [6,7]. In order to test the applied programs, diffusion profiles were calculated by DIFFUSEDC using a given $D(C)$ and then

* Corresponding author. Tel.: +49-89 3299 2228; fax: +49-89 3299 2279.

E-mail address: klaus.schmid@ipp.mpg.de (K. Schmid).

0022-3115/02/$ - see front matter
PII: S0022-3115(02)00807-3

Boltzmann–Matano analysis was utilized to these depth profiles to reproduce the $D(C)$. These tests also revealed where numerical instabilities are to be expected when using Boltzmann–Matano analysis to determine $D(C)$.

2. Theoretical considerations

2.1. DIFFUSEDC

The program DIFFUSEDC solves the general one-dimensional diffusion equation using a direct finite difference scheme. Starting from Fick's second law:

$$\frac{\partial C(x,t)}{\partial t} = \frac{\partial C(x,t)}{\partial x}\frac{\partial D(x,t)}{\partial x} + D(x,t)\frac{\partial^2 C(x,t)}{\partial x} \quad \text{with } D(x,t) \equiv D(C(x,t)) \tag{1}$$

and by using the following expressions for the first and second derivatives:

$$\frac{\mathrm{d}C(x,t)}{\mathrm{d}x} = \frac{C(x+\Delta x,t) - C(x-\Delta x,t)}{2\Delta x}, \tag{2}$$

$$\frac{\mathrm{d}C(x,t)}{\mathrm{d}t} = \frac{C(x,t+\Delta t) - C(x,t)}{\Delta t}, \tag{3}$$

$$\frac{\mathrm{d}C(x,t)^2}{\mathrm{d}x^2} = \frac{C(x+\Delta x,t) - 2C(x,t) + C(x-\Delta x,t)}{\Delta x^2}, \tag{4}$$

the diffusion equation can be expressed in terms of finite differences:

$$\frac{C(x,t+\Delta t) - C(x,t)}{\Delta t} = \frac{D(x+\Delta x,t) - D(x-\Delta x,t)}{2\Delta x}\frac{C(x+\Delta x,t) - C(x-\Delta x,t)}{2\Delta x} + D(x,t)\frac{C(x+\Delta x,t) - 2C(x,t) + C(x-\Delta x,t)}{\Delta x^2}. \tag{5}$$

By solving the above equation for $C(x,t+\Delta t)$ one can easily calculate the time evolution of a depth profile. Special care has to be taken for the $\Delta t/\Delta x^2$ ratio, in case it is too large (>0.5) the code becomes instable regarding the occurrence of oscillations. This is a problem typical for direct finite difference approaches and was already documented in [8]. Special boundary conditions have to be taken into consideration at the surface namely how to calculate $C(x-\Delta x,t)$ since this value lies outside the surface. In the case of C in W the surface is considered to be an infinite diffusion barrier. No C is allowed to leave the surface since sublimation can be safely ignored in the temperature region of interest. This can be expressed by defining the flux off from the surface to be zero as in the following equation [5]:

$$\left.\frac{\mathrm{d}C(x,t)}{\mathrm{d}x}\right|_{x=0} \equiv 0. \tag{6}$$

$C(x-\Delta x,t)$ can be calculated from Eq. (6) after rewriting it in terms of finite differences:

$$\left.\frac{C(x+\Delta x,t) - C(x-\Delta x,t)}{2\Delta x}\right|_{x=0} \equiv 0, \quad \text{bzw.} C(x-\Delta x,t)|_{x=0} = C(x+\Delta x,t)|_{x=0} = C(\Delta x,t). \tag{7}$$

2.2. Boltzmann–Matano analysis

The diffusion coefficient in a concentration gradient depends on the local concentration of the elements [9]. To determine this effective concentration dependent diffusion coefficient $D(C)$, a Boltzmann–Matano analysis has been used for a long time [6,7]. Most publications give only the final formula for $D(C)$ but to see the limitations of this method this paper will give a short overview of the derivation and special boundary conditions that have to be met in order for this method to be applicable. By applying the following variable transformation $\eta = x/\sqrt{t}$ to the diffusion equation (1) and by assuming that $C(x,t) \equiv C(\eta)$ one can rewrite

$$-\frac{\eta}{2}\frac{\mathrm{d}C}{\mathrm{d}\eta} = \frac{\mathrm{d}}{\mathrm{d}\eta}\left(D(C)\frac{\mathrm{d}C}{\mathrm{d}\eta}\right). \tag{8}$$

After canceling $\mathrm{d}\eta$, dividing by $\mathrm{d}C$ and integrating by $\int_{C_1}^{C_2}\mathrm{d}C$ one gets

$$-\frac{1}{2}\int_{C_1}^{C_2}\eta\,\mathrm{d}C = \left[D(C)\frac{\mathrm{d}C}{d\eta}\right]\Bigg|_{C_1}^{C_2} \tag{9}$$

with C_1, C_2 are two concentrations of $C(x,t)$. Eq. (9) can be rewritten in terms of x and t as

$$\int_{C_1}^{C_2} x(C)\,\mathrm{d}C = -2t\left\{D(C)\frac{\mathrm{d}C}{\mathrm{d}x}\bigg|_{C_2} - D(C)\frac{\mathrm{d}C}{\mathrm{d}x}\bigg|_{C_1}\right\}. \tag{10}$$

When $\frac{\mathrm{d}C}{\mathrm{d}x}\big|_{C_2} \equiv 0$, D at concentration $\overline{C}$ can be written as

$$D(\overline{C}) = \frac{1}{2t\frac{\mathrm{d}C}{\mathrm{d}x}\big|_{\overline{C}}}\int_{\overline{C}}^{C_2} x(C)\,\mathrm{d}C. \tag{11}$$

For Eqs. (9) and (10) to be valid, x ranges from $-\infty$ to $+\infty$ and $x = 0$ defines a plane such that

$$\int_0^{C_2} x(C)\,\mathrm{d}C \equiv 0 \tag{12}$$

is fulfilled. The thereby defined surface is called 'Matano interface' and can be interpreted as the requirement of conservation of mass. Namely every depletion to the left side of the interface must be compensated by an accumulation to the right side. For the Matano interface to

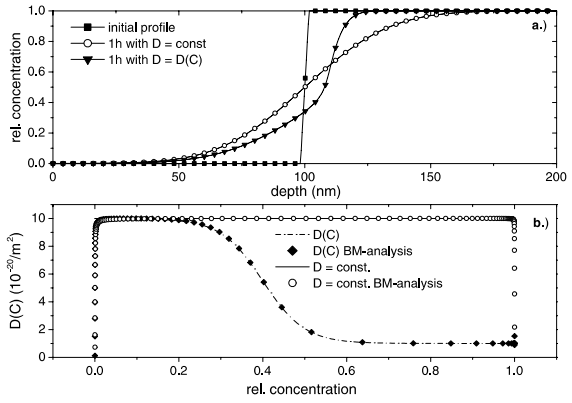

Fig. 1. (a) Simulated depth profiles calculated by DIFFUSDC for $D = \text{const.}$ and $D = D(C)$. (b) The results for $D(C)$ obtained from Boltzmann–Matano analysis of the profiles from (a) are compared to of $D(C)$ used in the simulation.

be just a straight plane the following initial boundary conditions must be fulfilled prior to diffusion:

$$C = C_0 \quad \text{for } x < 0, t = 0, \text{ i.e. } C = C_0 \quad \text{for } \eta = -\infty,$$
$$C = 0 \quad \text{for } x > 0, t = 0, \text{ i.e. } C = 0 \quad \text{for } \eta = \infty. \tag{13}$$

This means that the diffusion couple used should have a sharp interface in order to fulfill these conditions such as an evaporated W layer on pure C. In addition the sample must be infinite in both $+x$ and $-x$ directions. For a real world C/W diffusion couple this means that the carbon must not completely penetrate through the W layer.

If all boundary conditions are met the method reproduces the correct $D(C)$ as can be seen in Fig. 1. In Fig. 1(a), the depth profiles resulting from two DIFFUSEDC calculations are shown one for $D = \text{const.}$ and one for a D depending on the concentration. In Fig. 1(b), the actual values of $D(C)$ used for the calculation are compared to the result from the BM-analysis. One can see the very good match between the actual and the reproduced values in both cases. Larger deviations only occur at the boundaries of the concentration range. This is due to numerical inaccuracies in the calculation of the integral and the derivatives at the boundaries. At these concentrations both the integral and the derivative approach zero and the accuracy suffers from the ratio of two very small numbers.

3. Experimental

3.1. Sample preparation

The results presented here were gathered during four experimental campaigns partly differing in the type of C-substrate used and in the thickness of the W layer. In all four campaigns pyrolytic graphite was used which was cut in parallel to the graphite planes during the first and the second campaigns and perpendicular to the planes during the third and fourth campaign. Prior to the application of the W layer all C substrates were polished to $\approx$0.1 μm surface roughness in order to achieve a good depth resolution at the C/W interface in the Rutherford backscattering spectroscopy (RBS) measurement. During the first, third and fourth campaign the nominal thickness of the polycrystalline W layer was 100 nm created using magnetron sputtering. During the second campaign a 190 nm polycrystalline W layer was evaporated. The process parameters for preparation of the magnetron sputtered samples were: power 100 W, temperature 473 K, Ar-pressure 0.40 Pa, deposition time 7 min. X-ray .reflection analysis of the samples showed that the density of the layers was 99% of the W single crystal density. A detailed description of the magnetron sputtering apparatus can be found in [10,11]. An XPS analysis of the samples prior to the heating steps showed that oxygen was the main impurity with concentrations of $\approx$5% in the sputtered samples and $\approx$20% in the evaporated samples.

The samples were heated from the rear (the side opposite to the W layer) by an electron beam heater in a vacuum chamber with a pressure of 5×10^{-6} Pa. The temperature was measured using an infrared pyrometer which was calibrated at 1073 K with an optical pyrometer. The emissivity used for the measurement with the optical pyrometer was taken from [12]. It was that the emissivity would not change in the temperature range from 1000 to 1100 K.

3.2. Depth profiles

The depth profiles were measured by means of RBS using 2 MeV ^{4}He ions except for the second campaign, where 1.5 MeV ^{7}Li ions were used. A typical RBS spectrum obtained during the third campaign is depicted in Fig. 2. The W part of the spectrum shown is as obtained before and after heating for 4 and 8 h at 1073 K. One can clearly see how carbon diffuses into the W layer, thereby reducing the W peak height. The depth profiles were extracted from the backscattered energy distribution using Bayesian statistical analysis [13]. The required apparatus function was extracted from the high energy edge of a W RBS spectrum. In an iterative procedure the RBS spectra were simulated for given depth distributions and the best fit was chosen on the basis of Bayesian probability theory [13]. In Fig. 3, the result of this procedure is compared for data from the third campaign at 1073 K with the best fit of distributions from the RBS-simulation code SIMNRA [14] as chosen by hand. In most cases the agreement between the two methods is excellent. The deviations between the two results in Fig. 3

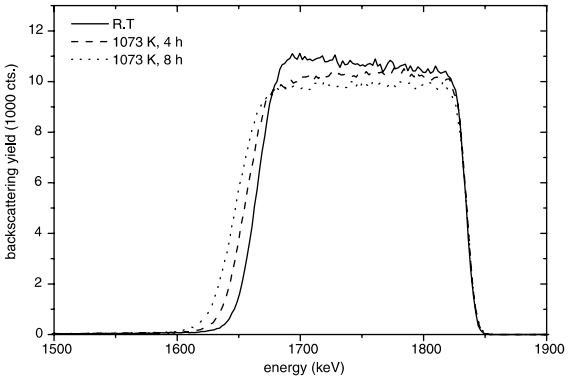

Fig. 2. Typical RBS spectrum using 2 MeV ^{4}He obtained during the third experimental campaign.

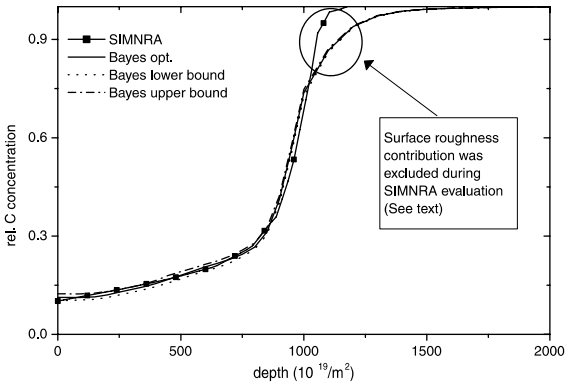

Fig. 3. Comparison of a Bayes and SIMNRA based evaluation of an RBS measurement.

at a depth of $\approx 1000 \times 10^{19}$ m^{-2} result from the surface roughness at the C/W interface which is misinterpreted by the RBS model used in the Bayesian analysis. The region of the spectra affected by these artifacts was determined from the RBS spectra of an unheated sample and was then not taken into account during the SIMNRA evaluation hence the difference compared to the Bayesian analysis. These artifacts obscure the transition from the W layer to the C substrate in the concentration range from 85% C to 100% C. This inflicts an upper limit of 85% C for the considered concentration range for $D(C)$. A lower concentration limit of $\approx$10% C for the obtainable $D(C)$ is determined by the numerical inaccuracies that were mentioned in Section 2.2.

From either program one obtains a relative C concentration depth profile with the depth scale in atoms/m^2. In order to extract diffusion coefficients in units of (m^2/s) one has to divide this length scale by the local number density, n (atoms/m^3) in order to obtain the depth in m. The density usually depends on the relative concentrations of the constituents present at a certain depth interval.

Assuming that the atomic volume

$$v_i = \frac{1}{n_i} \tag{14}$$

of the constituents in the mixture is the same as in the pure material one can calculate the number density of the mixture from

$$\frac{1}{n} = \sum \frac{C_i}{n_i}, \tag{15}$$

where n_i and C_i are the number density of the pure material and the relative concentration of component i, respectively. With the assumption of constant atomic volume an error is introduced into the depth profile since the true density is usually affected by chemical bond formation. For example tungsten monocarbide has a density of 15.36 Mg/m^3 corresponding to 4.7×10^{28} WC/m^3. Eq. (15) yields a density of 4.1×10^{28} WC/m^3 corresponding to an error of $\approx$10%. The average width of a depth interval used to define the depth profile for the simulation is $\approx$5 nm and on average each profile consists of 50 intervals. An ΔW error of 10% in the interval width results in an error of the intervals depth position of $i\Delta W$. With 50 intervals and a $\Delta W \approx 0.5$ nm this yields an error of $\approx \pm 25$ nm for the deepest layer. For illustration the resulting error bars are depicted in Fig. 4 showing the depth profiles from campaign 1. This error represents an upper limit since for C concentration close to zero or unity the local number density is that of pure W or of pure C, respectively, which are known from literature.

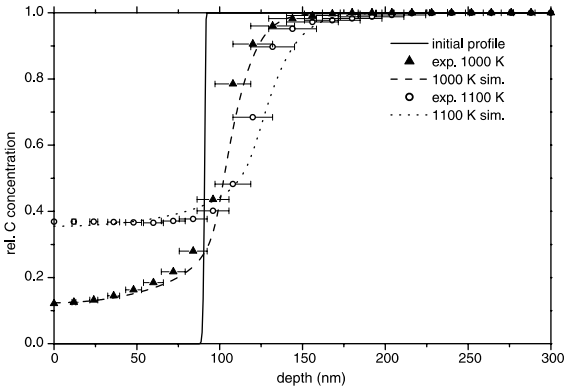

Fig. 4. RBS C-depth profiles obtained during the first experimental campaign together with the profiles calculated by DIFFUSEDC during the fitting procedure.

4. Results

4.1. $D(C)$ from fitting

During the first campaign a single diffusion couple was heated in three consecutive steps at 800, 1000 and 1100 K for 16 h each. Prior to the first and after each of the following heating steps the depth profile of C diffused into the W layer was determined. No diffusion could be found within the depth resolution of the RBS measurement after the 800 K heating step. The obtained depth profiles at higher temperatures are illustrated in Fig. 4. Since the diffusing C has reached the W surface for all temperatures above 800 K, the target could no longer be treated as 'infinite' and the BM-analysis could not be applied. Therefore, the concentration dependent effective diffusion coefficient was determined by simulating the depth profile with DIFFUSEDC and iteratively adjusting $D(C)$. As it was expected that the diffusion coefficient $D(C)$ varies smoothly from a value D_0 at low to a value D_1 at high C concentrations the functional dependence of D on C was expressed by a Boltzmann function, Eq. (16). There C_0 expresses the position and dc the steepness of the transition from D_0 to D_1

$$D(C) = \frac{D_0 - D_1}{1 + \exp\left(\frac{C - C_0}{\mathrm{dc}}\right)} + D_1. \tag{16}$$

The depth profiles as simulated by the DIFFUSEDC code using the obtained $D(C)$are also shown in Fig. 4 and fit the experimental values quite well. The values for $D(C)$ used for the simulations are depicted in Fig. 5. They all exhibit a sharp drop for a certain C concentration C_0 which seems to increases with temperature. Simply choosing a principle shape of $D(C)$ and using it to fitt depth profiles introduces a certain ambiguity. In order to verify the results we launched three additional experimental campaigns.

4.2. $D(C)$ from Boltzmann–Matano analysis

In the second campaign a sample was heated for 2 and 6.5 h at 1030 K, i.e. for a total of 8.5 h. The heating was performed in two steps because it was then possible to compare the results obtained for $D(C)$ after each step. They should be equal since in the present model the diffusion coefficient does not depend on heating time. Great care was taken to fulfill the initial boundary conditions in Eq. (13). It was also important that no carbon would diffuse up to the surface since then the W layer could no longer be treated as infinite and BM-analysis could not be applied. Again after each heating step the C-depth profiles were determined by RBS, the results are shown in Fig. 6. Then $D(C)$ was determined from the depth profiles by applying Boltzmann–Matano analysis and these results are depicted in Fig. 7. The $D(C)$ results obtained after different heating times at the same temperatures agree quite within the scatter of the data. The principal shape of $D(C)$ is similar to that assumed during the first campaign (Section 4.1). The scattered structure of the $D(C)$ values results from the fact that the BM-analysis is sensitive to the derivative of the depth profiles which does not change smoothly due to the spatial discreteness of the depth profile resulting from the evaluation procedure.

In the third campaign a single sample was heated in two consecutive steps for 4 h i.e. in total 8 h at 1073 K. During the second heating step the C depth profile eventually reached the surface and due to reasons mentioned above the Boltzmann–Matano analysis could only be applied to the profile obtained after the first heating step. In order to be able to test this result we used $D(C)$ values from the first heating step to simulate

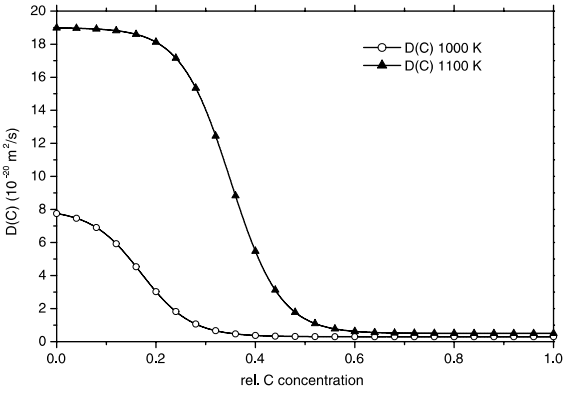

Fig. 5. $D(C)$ values obtained during the iterative fitting procedure. The depth profiles calculated by DIFFUSEDC using these values are depicted in Fig. 4.

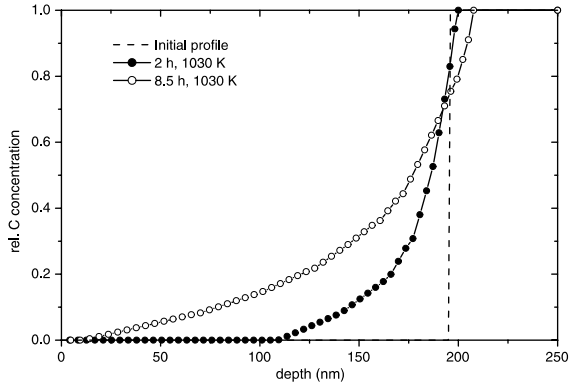

Fig. 6. RBS C-depth profiles obtained during the second experimental campaign.

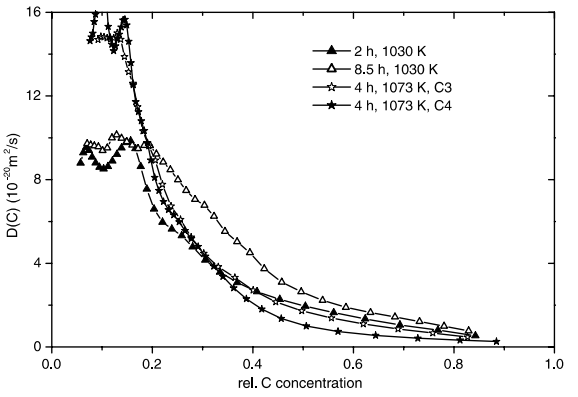

Fig. 7. Resulting $D(C)$ from Boltzmann–Matano analysis of depth profiles from the second, third and fourth experimental campaigns.

the depth profile obtained after the second heating period and see if the result fits the experimental data.

The measured depth profiles are shown in Fig. 8. One can clearly see that after the second heating period C has diffused through the W layer and now surface concentration of ≈10% is present. The DIFFUSEDC simulation of the second depth profile is also shown in Fig. 8. It is in good agreement with the experimental data corroborating that $D(C)$ is not dependent on the heating time. The fourth campaign was identical to the third one except that the diffusion couple was heated in only one step for 4 h at 1073 K. It was intended to test the reproducibility of the results of the third campaign. The resulting depth profile is depicted in Fig. 8 and is all most identical to the profile obtained during the third campaign. Therefore also the $D(C)$ extracted by BM-analysis which is shown in Fig. 7 reproduces the result from the third campaign.

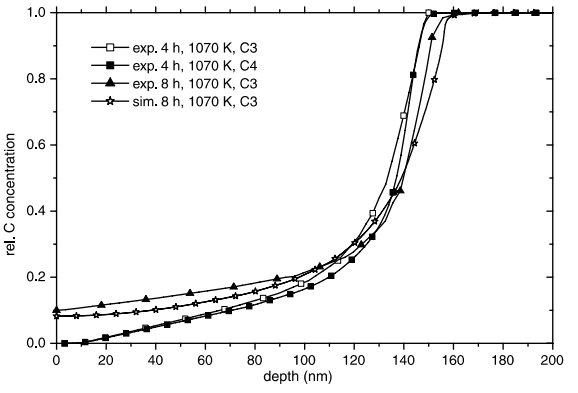

Fig. 8. Depth profiles measured during the third and fourth campaigns. Also shown is the simulation of the depth profile after 8 h at 1070 K using the $D(C)$ obtained from the first heating step.

5. Discussion

All depth profiles obtained during the first campaign show C diffusion up to the surface, where a flat depth profile develops which is well reproduced by the DIFFUSEDC calculations assuming a reflective boundary condition Eq. (7).

All obtained results for $D(C)$ exhibit the same principal shape as can be seen in Fig. 9. For low C concentrations the diffusion is large and of the order of 10^{-19} m^2/s but for high carbon concentrations diffusion is low in the order of 10^{-21} m^2/s. This can be understood by considering that by moving to higher C concentrations one moves from C diffusion in W to C diffusion in W_2C, WC and even graphite, where the diffusion coefficient according to [15] is negligible in the considered temperature range.

The diffusion coefficient calculated in this work is the so-called interdiffusion coefficient which reflects the average of the overall movement of all constituents diffusing in a concentration gradient. Earlier publications on the diffusion of C in W in contrast give the tracer or chemical diffusion coefficient of C in W. The general relation between interdiffusion coefficient $D(C)$ and tracer diffusion coefficients for a two component system is given by Eq. (17). The details of its derivation can be found in [9]

$$D(C_1, C_2) = (D_1^* C_2 + D_2^* C_1)\left(1 + \frac{\mathrm{d}\ln\gamma_1}{\mathrm{d}\ln C_1}\right). \tag{17}$$

Here γ_1 is the activity coefficient of component 1, C_i are the relative concentrations and D_i^* are the tracer diffusion coefficients. By using the fact that $C_2 = 1 - C_1 \equiv 1 - C$ one can write

$$D(C_1, C_2) = (D_1^*(1 - C_1) + D_2^* C_1)\left(1 + \frac{\mathrm{d}\ln\gamma_1}{\mathrm{d}\ln C}\right). \tag{18}$$

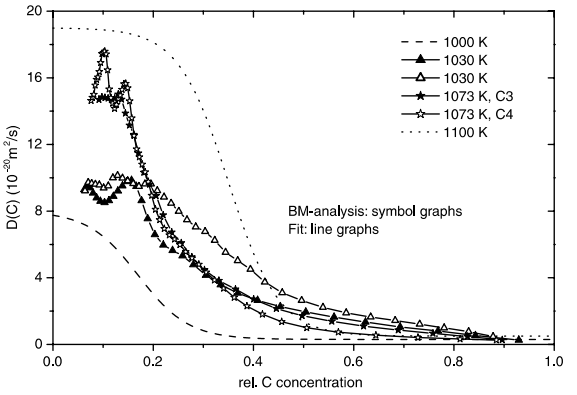

Fig. 9. Comparison of all $D(C)$ results obtained from Boltzmann–Matano analysis and fitting of depth profiles.

This equation states that if γ is constant as it is the case for a dilute or ideal solution (i.e. $\Delta G_{\mathrm{mix}} = 0$) the diffusion coefficient is just a linear combination of the tracer diffusion coefficients. If ΔG_{mix} is not zero, i.e. a miscibility gap occurs, D does depend on the concentration in a non-linear way governed by the dependency of γ on the concentration. A miscibility gap occurs in the case for C in W for C concentrations that exceed the order of a few percent and therefore a non-linear dependence of D on C can be expected. Also this means that the dependence on the concentration can in general not be neglected during modeling diffusion of C in W. The principal shapes found here are typical for the variation of $D(C)$ across a binary phase diagram as can be seen in [16].

The transition between the high and low $D(C)$ regimes is situated in the concentration range from 20% to 40% depending on the temperature and is a measure for the maximum concentration of C in W with high mobility. In [3,17] the authors investigate the formation of different carbides while heating C layers on W substrates. They find the formation of W_2C at about 1000 K and a transition to WC when moving to higher (>1200 K) temperatures. As known from literature [18] the W_2C phase is less stable than the WC phase below 1500 K. They therefore attribute the formation of the less stable W_2C phase to the fact that at these low temperatures diffusion is still to low to allow high enough concentrations of C in W (within heating times of several hours) for the formation of the more stable WC phase. At higher temperatures the diffusion is strong and a large enough carbon concentration results in the formation of WC. A comparison of the results from [3] and [17] with the position of the transition point in this work allows the correlation of the concentration dependence of the diffusion coefficient with the onset of the formation of the different carbides.

At ≈1000 K the concentration at the transition point is about 20% which is similar to the stoichiometry of tungsten dicarbide W_2C which according to [3] and [17] is formed at that temperature. The transition point shifts to approximately 40% at 1100 K which corresponds approximately to the stoichiometry of tungsten monocarbide WC which is formed at about 1100 K according to [3] and [17]. Therefore this concentration mobility threshold can be correlated with the formation of carbides which in the case of WC requires the C atoms to diffuse to interstitial binding sites. At C concentrations exceeding this threshold the C atoms then have to diffuse through a tungsten carbide phase with a very low diffusivity [4].

The comparison of $D(C)$ with literature values for the diffusion coefficient D cannot be done directly as seen from Eq. (18). One could only compare the $D(C)$ for very small concentrations but even then $D(C)$ should be reduced compared to the tracer diffusion coefficients from literature due to the formation of carbides which

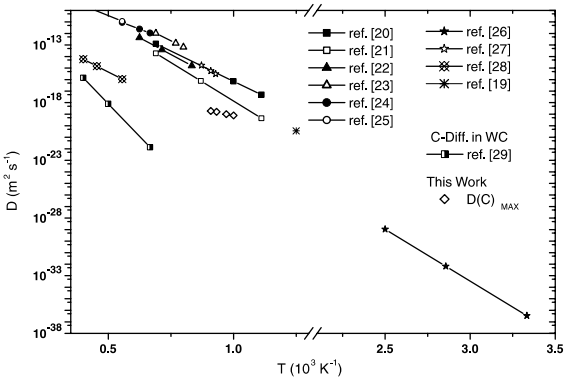

Fig. 10. Comparison of the values for the diffusion coefficient of this work with literature values [20–29]. The maximum values for $D(C)$ obtained at low C concentrations are plotted in an arrhenius plot.

can be understood to act as traps. Therefore, one would expect the maximum values of $D(C)$ from this work to be situated somewhere between the tracer diffusivities of C in W and in WC. This can be seen in Fig. 10 where literature values from [4] are compared to the $D(C)$ results from this work for low C concentrations. One can see that literature data is quite scattered and that the low concentration values of $D(C)$ obtained here lie between the literature data for diffusion of C in W and in WC. A possible reason for the scatter is the dependence of the diffusion coefficient on the sample structure. The samples used in the literature data summarized in Fig. 10 range from polycrystalline wires to pressed powder particles, hence differences in the diffusion coefficient are to be expected. In Ref. [19] the interdiffusion coefficient for C in W is determined in a very indirect way from simulations of the erosion of W during C bombardment but similar values as in this work were obtained. A diffusion coefficient of 3.6×10^{-21} m^2/s was found at ≈800 K which fits the values found here when extrapolating to lower temperatures.

6. Conclusions

The diffusion of carbon in W has been found to depend strongly on the carbon concentration. The effective concentration dependent diffusion coefficient $D(C)$ of C in W was determined in the temperature range from 1000 to 1100 K. Two independent methods were used which gave similar results. For adequate boundary conditions the Boltzmann–Matano analysis was applied and in cases where this approach was not feasible the carbon depth profiles were fitted iteratively. For this fitting procedure a new program DIFFUSEDC was developed and successfully tested to solve numerically the diffusion equation with a concentration dependent diffusion coef-

ficient. The results for $D(C)$ exhibit a sharp drop for a temperature dependent relative C concentration which can be correlated with the onset of formation of different tungsten carbides. The maximum diffusion coefficients were found at low C concentrations below 15% and are in the order of magnitude of 10^{-20}–10^{-19} m^2/s, in good agreement with literature values.

Acknowledgements

The authors would like to thank Walter Ottenberger and Arno Weghorn for valuable technical assistance and Udo v. Toussaint and Rainer Fischer for help with the Bayesian analysis of the RBS spectra. Also we would like to thank Tilo Druesedau for preparing and characterizing the magnetron sputtered layers.

References

[1] R. Pugno, A. Kallenbach, J. Nucl. Mater. 290–293 (2001) 308.
[2] ITER physics basis, Nucl. Fusion 39 (1999) 2391.
[3] J. Luthin, C. Linsmaier, Surf. Sci. 454–456 (1948) 78.
[4] Gmelin Handbook of Inorganic and Organometallic Chemistry, Tungsten, Supplement vol. A5b, Springer, Berlin, 1993.
[5] J. Crank, The Mathematics of Diffusion, Oxford University, Oxford, 1975.
[6] A. Sultan, S. Bhattacharya, S. Batra, S. Banerjee, J. Vac. Sci. Technol. B 12 (1998) 391.
[7] M. Snabl, M. Ondrejcek, J. Chem. Phys. 108 (1998) 4212.
[8] P. Harrison, Phy. Stat. Sol. b 197 (1996) 81.
[9] R.J. Borg, G.J. Dienes, An Introduction to Solid State Diffusion, Academic Press, New York, 1988.
[10] F. Klabunde, M. Löhmann, J. Bläsing, T. Drüsedau, J. Appl. Phys. 80 (11) (1996) 6266.
[11] M. Löhmann, F. Klabunde, J. Bläsing, P. Veit, T. Drüsedau, Thin Solid Films 342 (1999) 127.
[12] L. David, H.P.R. Frederikse, CRC-Handbook of Chemistry and Physics, 75th Ed., CRC, Boca Raton, FL, 1994.
[13] U. Toussaint, R. Fischer, K. Krieger, V. Dose, New J. Phys. 1 (1999) 11.1.
[14] M. Mayer, MPI f. Plasmaphysik Technical report IPP 113 (9).
[15] M.A. Kanter, Phys. Rev. 107 (1957) 655.
[16] C. Birchenall, Atom Movements, ASM, Cleveland, 1951.
[17] J. Luthin, C. Linsmaier, PhD thesis, Bayreuth, 2000.
[18] I. Barin, Thermochemical Data of Pure Substances, VCH, 1986.
[19] W. Eckstein, V.I. Shulga, Nucl. Instrum. Meth. B 153 (1999) 415.
[20] V.Y. Shchelkonogov, Elektron. Svoistva Tverd. Tel. Fazovye Prevrashch. (1978) 115, Chem. Abs. 94 (1981), 19276.
[21] L.N. Aleksandrov, Int. Chem. Eng. 3 (1963) 108.
[22] A.I. Nakonechnikov, L.V. Pavlinov, V.N. Bykov, Phys. Met. Metallogr. 22 (1966) 73.
[23] L.N. Aleksandrov, V. Shchelkonogov, Soviet Powder Metall. Met. Ceramic. (1964) 288.
[24] A. Shepela, J. Less-Common Met. 26 (1972) 33.
[25] I. Kovenskii, Diffus. Body Cent. Cubic Met. Pap. Int. Conf., Gatlinburgh, TN, 1964, p. 283.
[26] V. Shchelkonogov, L. Aleksandrov, V. Piterimov, V. Mordyuk, Phys. Met. Metallogr. 25 (1968) 68.
[27] K. Rawlings, S. Foulias, B. Hopkins, Surf. Sci. 109 (1981) 513.
[28] A. Piquet, G. Pralong, H. Roux, Surf. Sci. 109 (1981) 513.
[29] A.E.G.V. Samsonov, A.L. Burykina, Zashch. Pokrytiya Met. 6 (1974) 5.